The influence of resolution recovery by using collimator detector response during 3D OSEM image reconstruction on ^{99m}Tc-ECD brain SPET images

Faraz Kalantari[1] PhD, Hossein Rajabi[1] PhD, Mohammad Reza Ay[2,3,4] PhD, Sied Kazem Razavi-Ratki[4] MD, Armaghan Fard-Esfahani[4] MD, Davood Beiki[4] MD, Mohammad Eftekhari[4] MD, Babak Fallahi[4] MD, Leila Sadeghian[4] MD, Alireza Emami-Ardekani[4] MD

1. Department of Medical Physics, Tarbiat Modares University, Tehran, Iran
2. Research Center for Science and Technology in Medicine and
3. Department of Medical Physics and Biomedical Engineering and
4. Research Institute for Nuclear Medicine, Tehran University of Medical Sciences, Tehran, Iran

***

Keywords: SPET -Resolution – Brain ^{99m}Tc-ECD SPET – Image resolution – Image reconstruction – Iterations

Correspondence address:
Alireza Emami-Ardekani MD
Research Institute for Nuclear Medicine, Tehran University of Medical Sciences, Tehran, Iran
Email: emami_a@sina.tums.ac.ir
Tel : +9821 88633333

Received:
5 March 2012
Accepted revised:
30 April 2012

Abstract

Partial volume effect, due to the poor spatial resolution of single photon emission tomography (SPET), significantly restricts the absolute quantification of the regional brain uptake and limits the accuracy of the absolute measurement of blood flow. *In this study* the importance of compensation for the collimator-detector response (CDR) in the technetium-99m ethyl cysteinate dimer (^{99m}Tc-ECD) brain SPET was assessed, by incorporating system response in the ordered-subsets expectation maximization (OSEM) reconstruction algorithm. By placing a point source of ^{99m}Tc at different distances from the face of the collimator, CDR were found and modeled using Gaussian functions. A fillable slice of the brain phantom was designed and filled by ^{99m}Tc. Projections acquired from the phantom and also 4 patients who underwent the ^{99m}Tc-ECD brain SPET were used in this study. To reconstruct the images, 3D OSEM algorithm was used. System blurring functions were modeled, during the reconstruction in both projection and backprojection steps. *Our results* were compared with the conventional resolution recovery using Metz filter in filtered backprojection (FBP). Visual inspection of the images was performed by six nuclear medicine specialists. Quantitative analysis was also studied by calculating the contrast and the count density of the reconstructed images. For the phantom images, background counts and noise were decreased by 3D OSEM compared to the FBP-Metz method. Quantitatively, the ratio of the counts of the occupied hot region to that of the cold region of the reconstructed by FBP-Metz images was 1.14. This value was decreased from 1.12 to 0.86 for 3D OSEM of 2 and 30 iterations respectively. The reference value was 0.85 for the planar image. For clinical images, hot to cold regions (grey to white matter), the count ratio was increased from 1.44 in FBP-Metz to 3.2 and 4 in 3D OSEM with 10 and 20 iterations respectively. Based on the interpretability of images, the best scores (3.79±0.51) by the physicians were given to the images reconstructed by 3D OSEM and 10 iterations. This value was 0.63±0.77 for FBP-Metz images. *In conclusion*, by incorporating the distance dependent CDR during 3D OSEM, it was possible to reconstruct the brain images with much higher resolution and contrast as compared to the conventional resolution recovery method, which used FBP-Metz. It was however important to make a trade-off between noise and resolution by determining an optimum iterations number.

Hell J Nucl Med 2012; 15(2): 92-97 *Epub ahead of print: 27 June 2012* *Published on line: 27 June 2012*

Introduction

Technetium-99m-ethyl cysteinate dimer (^{99m}Tc-ECD) SPET is extensively used as a clinical tool for the assessment of the regional cerebral blood flow (rCBF) [1, 2]. Quantitative brain SPET has a well-established role in the diagnostic evaluation of perfusion abnormalities of the brain SPET in patients with temporal lobe epilepsy [3, 4], traumatic brain injuries [5, 6], Alzheimer's disease, and dementias [7, 8]. The spatial resolution should be adequate to show small brain structures like thalamus and basal ganglia. Basal ganglia and putamen have a remarkable clinical impact and should be evaluated carefully. Brain uptake is high in the subcortical gray matter, the basal ganglia and thalamus [9, 10]. On the transverse images with the optimal spatial resolution, globus pallidus and putamen seem like a triangular structure and the caudate nucleus should be seen as a small protuberance on the margin of the basal ganglia. The internal capsule located between the thalami and basal ganglia has a little uptake on the cerebral perfusion imaging and thalamus is seen as a separate structure.

Quantitative accuracy of the brain perfusion SPET images is degraded by the photon attenuation [11-13], scattered photons [14-16] and by distance dependent collimator detector response [17]. Moreover, statistical noise and background radiations degrade the images. Beside these factors that influence image quality, there are also issues associated

with the selection of the image reconstruction algorithm, filter parameters, and compensation methods [18-22].

It has been shown that for the brain SPET, attenuation can be successfully corrected by applying the Chang's algorithm and considering the uniform attenuation coefficients after image reconstruction [13, 21, 23]; however there are studies that show a small improvement of the CT-based non-uniform attenuation correction [21, 22, 24]. Scatter correction can be successfully applied using dual or triple energy windows during or after image reconstruction [14, 21, 22, 24].

There are however challenges about the selection of the optimum method to compensate for collimator detector response (CDR). In a class of the conventional methods, the resolution recovery filters such as Metz or Wiener were used to compensate for the collimator and detector blurring using the inverse CDR in the frequency domain [25, 26]. The main advantage of this method is that it is fast and easy to implement. One important issue in applying the restoration filters is the selection of the CDR. Since CDR changes as a function of the distance, usually an average filter is used; for example, CDR for a distance from the face of the collimator equals to the radius of the rotation. Therefore, these filters will tend to overcompensate in the some parts of the image and undercompensate in other. Another issue associated with this method is that since Metz and Wiener filters use the inverse CDR, they are high-pass filters that amplify the noise and therefore it's necessary to make a trade-off between the degree of resolution recovery and the noise level. Metz filter is commercially available now on many SPET systems.

Other compensation methods are more accurate by incorporating the distance dependent CDR in the projector steps (forward and backward) of the iterative reconstruction algorithms [27-30]. This means that instead of forwarding the data in straight lines along the columns when calculating the projection value, the projector includes the probability for a photon to pass through the holes of the collimator. Due to the statistical nature of gamma rays emission in nuclear medicine, statistical reconstruction methods such as maximum likelihood expectation maximization (MLEM) or ordered subset expectation maximization (OSEM) that consider the Poisson nature of these data are often the iterative method of choice to be used for SPET image reconstruction [31, 32].

There are simulation studies that have evaluated the impact of resolution recovery by incorporating CDR during OSEM image reconstruction in the brain SPET images. They have used a digital phantom and analytical simulation to create the brain SPET projections [33]. Others employed Monte Carlo simulation and a digital brain phantom for the creation of SPET projections, but neglected the effect of photon attenuation and scattering [17]. They showed that resolution recovery by CDR modeling during OSEM, significantly reduce the effect of partial volume, increases the gray to white matter contrast and improves the accuracy of quantitative estimations.

In this research we used a physical brain phantom and real clinical images to assess the influence of the resolution recovery during image reconstruction on the quantitative accuracy of ^{99m}Tc-ECD brain SPET images via prototype study. We also compared our results with the conventional resolution recovery images using Metz filter.

Methods

Modeling CDR

A point source of 37MBq of ^{99m}Tc-pertechnetate was placed in different distances (5cm to 45cm with 5cm steps) from the face of the collimator. A total of four million counts were acquired for each distance in a 256X256 matrix with 1.35mm pixel size. Suitable 2D Gaussian functions were fitted on the CDR.

Phantom study

A single slice fillable phantom of the brain was designed and manufactured based on the ZUBAL digital phantom [34] and ^{99m}Tc-ECD bio-distribution; however, in this phantom all activities can be distributed in the gray matter only. Phantom size was 22cmX17cm with 1cm thickness. This phantom was filled with 150mL of ^{99m}Tc and water with an activity concentration of 74MBq.

Patient study

Previously acquired projections of the 4 patients (2 men and 2 women, aged: 34±7.4 years) who referred to our center for ^{99m}Tc-ECD brain SPET were used for image reconstruction. All patients had been intravenously injected by 925-1110MBq of ^{99m}Tc-ECD.

Data acquisition

Imaging was performed with a dual-head Symbia T2 gamma camera (Siemens Medical Solution Inc. USA) and low energy high resolution collimators. Tomography was performed using 120 stops at 30s per view in a 360° rotation. The crystal dimensions were 59.1X44.5cm, with a 9.5mm thickness. Approximately 4.5-5.0 million counts for the patients and 1.2 million counts for the phantom were acquired. The energy setting was 140keV with a 20% window. Image pixel size was 2.7mm in a 128X128 array.

Image reconstruction

Images were reconstructed using both the analytical FBP and 3D iterative OSEM algorithms with resolution recovery. The FBP reconstruction was done using Metz filter (cut-off: 0.25, order: 6) and Butterworth filter (cut-off: 0.22, order: 8). Parameters of these filters have been optimized for the acquired brain images in our department. The OSEM reconstruction was done using 1 to 30 iterations and 8 subsets per iteration. The 3D nature of CDR causes blurring across the multiple image slices, so in order to achieve a more accurate compensation, we must take into account this 3D effect. To achieve this goal, the image reconstruction must be done as a whole rather than a slice by slice. For any 3D estimation, blurring was done layer by layer for each of the planes based on their distances from the face of the collimator. After blurring our 3D estimation, the simple ray sum was applied to create the 2D mathematical projections. For the next projections, the activity phantom was rotated in its fixed grid. These mathematical projections were compared to the real projections. The error due to this comparison was backprojected to update the previous image. This process is repeated while the error reaches to a small and acceptable value [35].

Attenuation correction

Attenuation was corrected using Chang's first-order method (attenuation coefficient, μ=0.12cm^{-1}). The true value of μ for

the narrow beam is about 0.16cm^{-1}, however this value decreases due to the presence of the scattered photon. Therefore we used an effective attenuation coefficient which is about 0.12cm^{-1}. The Chang's method involves multiplication by a correction factor at each point of the image after the reconstruction. It has been shown that this algorithm can be applied successfully in uniform and symmetric organs such as the brain [13, 36, 37].

Evaluation parameters

Both the visual inspection and quantitative evaluation were used in this research. Visual inspection was done by six nuclear medicine specialists. They were asked to give scores between 0 and 4 (the best image) to the reconstructed images of FBP-Metz, 3D OSEM with 2, 6, 10 and 20 iterations based on interpretability, uniformity, and visibility of different parts of the brain scans such as the internal capsule, basal ganglia, and thalamus. For quantitative analysis, the mean counts in the grey and the white matter of the brain images were calculated as a function of the iteration number. The gray to white matter count ratio in the brain was also calculated for all the reconstruction methods. To achieve this goal, two regions of interest (ROI) were drawn in a uniform hot region and a uniform cold region near the first ROI.

In the phantom study, the ratio of the number of pixels in the hot region to the number of pixels in the cold region were determined for each reconstructed image. Count density was also calculated for each image. Higher count density means a thinner wall, less blurring, and better spatial resolution.

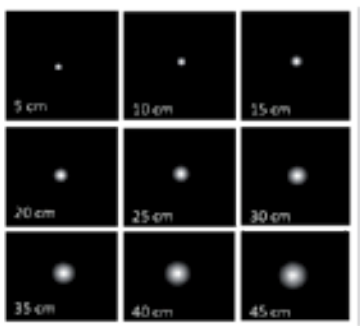

A

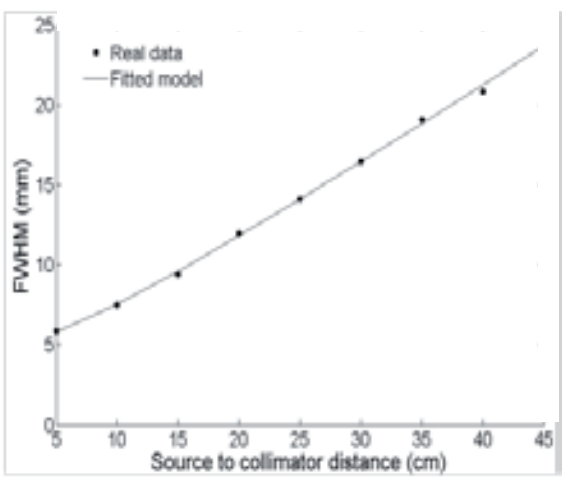

B

Figure 1. A: Images acquired from the point source of ^{99m}Tc at different distances from the face of the collimator, **B**: Plot of FWHM for CDR as a function of distance; the precision of fitted Gaussian model on the real data was R^2=0.991.

Results

CDR Modeling

As it has been shown in Figure 1, the full width at the half maximum (FWHM) of the Gaussian functions increased from 5.6mm to 24mm when the source to the collimator distance increased from 5cm to 45cm.

Phantom study

Figure 2 shows the reconstructed images by different algorithms: by FBP-Metz, FBP-Butterworth and 3D OSEM with the different iteration numbers. For all the reconstructed images by 3D OSEM, there was less background and noise compared to the images reconstructed by FBP-Metz. After 10 iterations, more details could be identified in the 3D OSEM compared with the FBP-Metz image. It was also obvious that there was a direct relation between image resolution and iteration numbers.

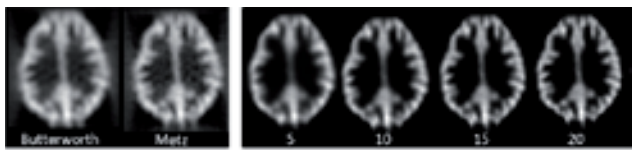

A B

Figure 2. Reconstructed images of the physical phantom by different algorithms; **A**: Filtrated back projection with Butterworth and Metz filter, **B**: 3D OSEM for the different iteration numbers.

In order to estimate image resolution, the ratio of the hot area to the cold area in each reconstructed image was compared with the reference image. A planar image of the phantom was acquired and used as the reference image. A simple threshold method was used to create the binary masks for each image. For each image, the hot region mask was created by defining a 30% of the maximum count. The rest of the image was considered as the cold region (Fig. 3). Figure 4, shows the ratio of the hot to the cold regions using the planar image as the reference image. The rest of the images were reconstructed by using different algorithms, as mentioned before.

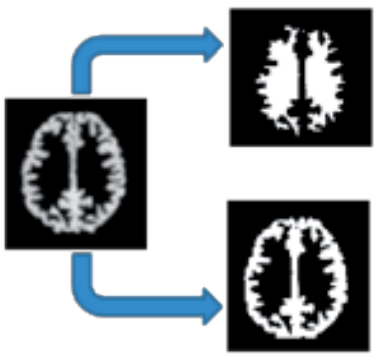

Figure 3. Creation of the binary masks for finding hot and cold areas by defining their threshold.

To evaluate the correction of partial volume effect, the mean pixel values in both the hot and cold regions were calculated for each image reconstructed by 3D OSEM with different iteration numbers. Regarding the phantom used, for an ideal image there should be no counts in the cold region and all counts should be observed in the hot region. As it has been shown in Figure 5, by increasing

the iteration number, the mean pixel value in the cold region was decreased. In contrast, by increasing the iteration number the mean pixel value in the hot region was increased.

Figure 4. The ratio of hot area to cold area using the planar image as reference. Other images were reconstructed by different reconstruction methods.

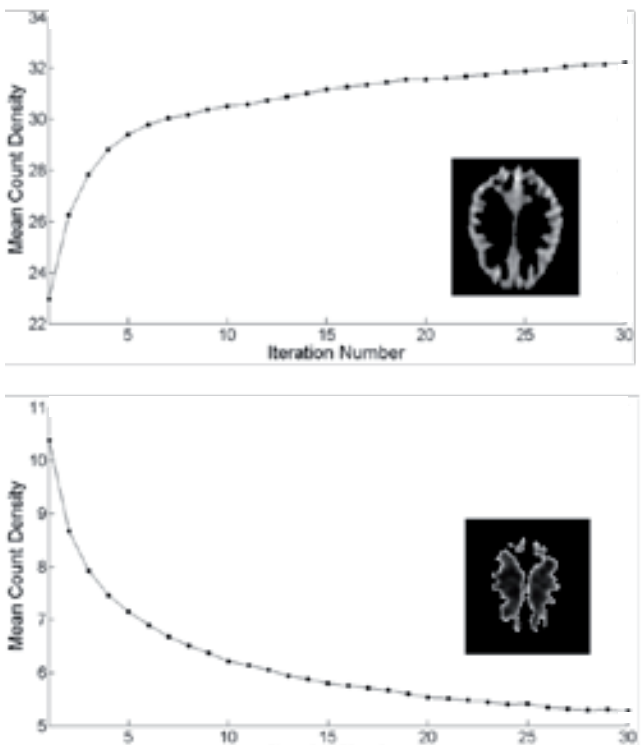

Figure 5. Variation of the mean count density in the hot (top) and the cold (bottom) regions versus the iteration number for images reconstructed by 3D OSEM.

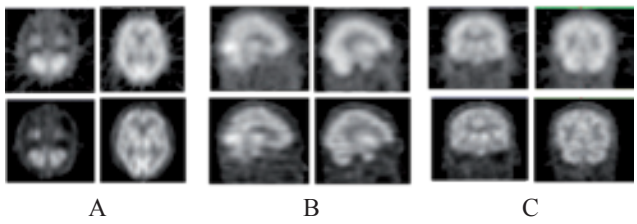

Figure 6. Two different sections of a real reconstructed brain image by FBP and Metz filter (top row) and by 3D OSEM with the resolution recovery and with 10 iterations and 8 subsets (bottom row) in three standard planes: **A**: transverse, **B**: sagittal and **C**: coronal.

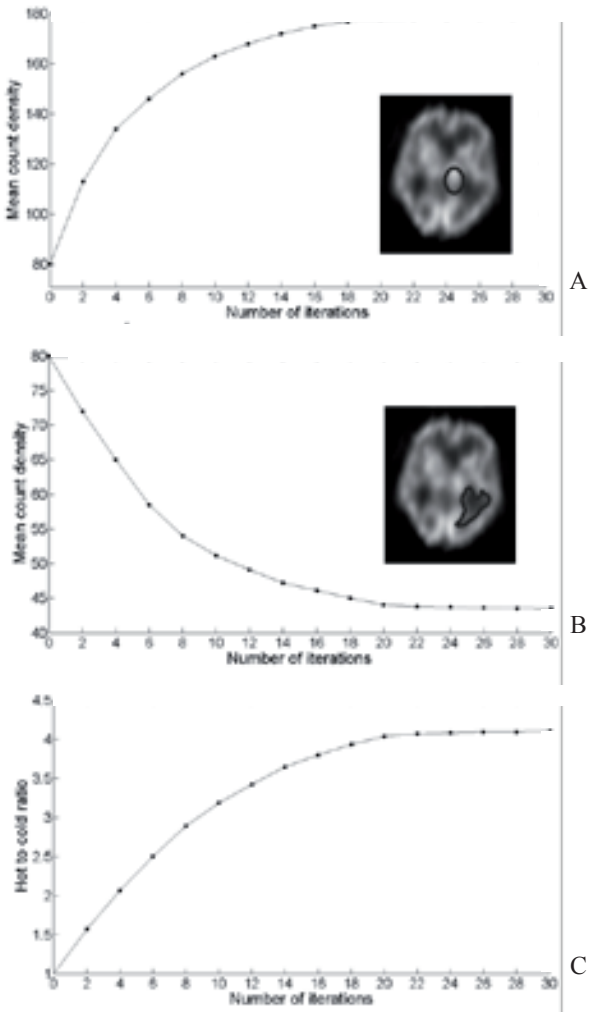

Figure 7. Variation of the mean count density in **A**: the hot, **B**: the cold regions and **C**: the hot-to-cold ratio of the brain image versus the iteration number.

Table 1. *The mean±standard deviation of scores for each patient and for all patients given by six nuclear medicine specialists in 0-4 scale*

Reconstruction method	FBP with Metz filter	3D OSEM 2 iterations	3D OSEM 6 iterations	3D OSEM 10 iterations	3D OSEM 20 iterations
Patient 1	0.50±0.83	0.67±0.52	3.00±0.63	3.67±0.81	2.17±0.75
Patient 2	0.50±0.83	0.67±0.52	2.83±0.41	3.83±0.41	2.17±0.98
Patient 3	0.67±0.81	0.83±0.75	3.00±0.63	3.83±0.41	1.67±1.03
Patient 4	0.83±0.75	0.33±0.52	3.00±0.63	3.83±0.41	2.00±0.63
All patients	0.63±0.77	0.63±0.58	2.96±0.55	3.79±0.51	2.00±0.83

Patient study

Figure 6 shows two different slices of the reconstructed image of a patient, reconstructed by both FBP with Metz filter as the conventional method of resolution recovery, and by 3D OSEM with CDR modeling. Ten iterations and 8 subsets per iteration have been used in 3D OSEM image reconstruction. It is obvious that much more structures can be distinguished in the image that has been reconstructed by the 3D OSEM method.

Two irregular regions of interest (ROI) were drawn in the hot and cold regions of the brain image in the transverse plane. As shown in Figure 7, by increasing the number of iterations, the mean count density in the hot region was increased (Fig. 7A). In contrast, the mean count density in the cold region by increasing the number of the iterations was decreased (Fig. 7B). Therefore the hot to cold region contrast was also increased (Fig. 7C). For both the hot and cold regions, however, the recovery curves reach a plateau after about 20 iterations. A single slice of an image reconstructed by Metz, and 3D OSEM with different iteration numbers can be seen in Figure 8.

Table 1 represents mean±standard deviation of the scores given to the each image by six nuclear medicine specialists. For each patient, between FBP-Metz and 3D OSEM with 2, 6, 10 and 20 iterations (all with 8 subsets), the best images were those reconstructed by using resolution, contrast, noise level and interpretability. The least scores were given by using FBP-Metz and 3D OSEM with 2 iterations.

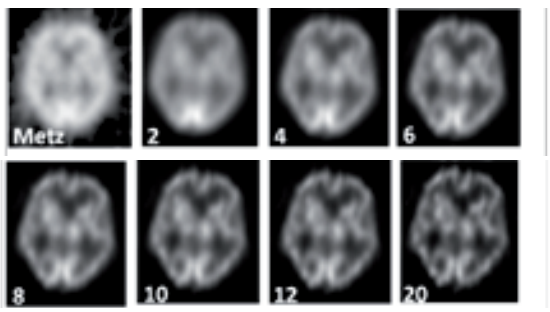

Figure 8. Images of a patient reconstructed by FBP-Metz and 3D OSEM with 2, 4, 6, 8, 10 and 20 iterations.

Discussion

Spatial resolution plays an essential role in the brain SPET images. Collimator and detector response are the main causes of loss of resolution in SPET images. There are some simulation studies that showed improvement of signal recovery by modeling CDR during brain image reconstruction. These studies reported an improvement up to 23% of the specific uptake ratio (SUR) [38, 39]. Others showed the superiority of 3D OSEM incorporating CDR over FBP [13, 40, 41]. Most of these studies have been performed on brain SPET images using iodine-123. The present study addressed quantitative and qualitative errors due to the poor spatial resolution in ^{99m}Tc-ECD SPET images. Since visual interpretation of brain SPET images is still the most common method of image interpretation, we evaluated the influence of 3D OSEM with CDR correction on image contrast and resolution.

The main advantage of using the phantom study was that we were aware of the true activity distribution and could use the phantom as a reference.

As shown in Figure 1, CDR is a function of the distance and the FWHM of the system response can vary from 5mm at the face of the collimator to 24mm at a distance of 45cm. This results in a non-uniform resolution in the final reconstructed image and adversely affects the quantitative accuracy of the brain images.

Conventional resolution recovery methods, use restoration filters such as the Metz filter; however, in these methods the 3D nature of CDR is neglected and the images are reconstructed slice by slice. The other disadvantage of using Metz filter is applying an average and constant filter and finally Metz filter amplifies noise that is considerable in higher frequencies. In 3D OSEM; however, it is possible to employ distance dependent CDR functions. Therefore we could reconstruct images with more precision. As shown in Figure 2, OSEM algorithm results in much better noise properties compared to FBP and Metz filters. The other advantage of OSEM algorithm is less background in the cold regions.

As shown in Figure 5, in the real brain images that contain the fewer counts, the recovery coefficients in both the hot and cold regions reach to their maximum after about 18 iterations. Therefore increasing the iteration numbers does not add useful information any more. Between the reconstructed images of 6 and 20 iterations, our specialists gave the highest score to the reconstructed images with 6 iterations. This shows the adverse effect of the noise on the interpretability of the images. Nowadays, many SPET systems are equipped with the resolution recovery programs [42, 43]. These softwares can improve the image resolution without any extra cost or additional imaging.

In conclusion, by incorporating the collimator dependant response during 3D OSEM images reconstruction on ^{99m}Tc-ECD brain SPET images, it has been possible to reconstruct brain images with higher spatial resolution and contrast, aiming to also achieve higher quantitative accuracy as compared to conventional resolution recovery method which used FBP-Metz. For that, it was important to make a trade-off between the noise and resolution by determining an optimum iteration number.

Acknowledgments

This research has been supported by Tehran University of Medical Sciences, under grant 89-03-58-11309, Tehran, Iran. The authors thank Dr. Mehrshad Abbasi, Dr. Mohsen Saghari and Dr. Saeed Farzanefar and for their kind collaboration in image interpretation.

The authors declare that they have no conflicts of interest.

Bibliography

1. Leveille J, Demonceau G, De Roo M et al. Characterization of technetium-99m-L,L-ECD for brain imaging perfusion , Part 2: Biodistribution and brain imaging in humans. *J Nucl Med* 1989; 30: 1902-10.
2. Vallabhajosula S, Zimmerman RE, Picard M et al. Technetium-99m ECD: a new brain imaging agent: in vivo kinetics and biodistribution studies in normal human subjects. *J Nucl Med* 1989; 30: 599-604.
3. Weil S, Noachtar S, Arnold S et al. Ictal ECD-SPECT differentiates between temporal and extratemporal epilepsy: confirmation by excellent postoperative seizure control. *Nucl Med Commun* 2001; 22: 233-7.
4. Grunwald F, Menzel C, Pavics L et al. Ictal and interictal brain SPECT imaging in epilepsy using technetium-99m-ECD. *J Nucl Med* 1994; 35: 1896-901.

5. Abdel-Dayem HM, Abu-Judeh H, Kumar M et al. SPECT brain perfusion abnormalities in mild or moderate traumatic brain injury. *Clin Nucl Med* 1998; 23: 309-17.
6. Abu-Judeh HH, Parker R, Singh M et al. SPET brain perfusion imaging in mild traumatic brain injury without loss of consciousness and normal computed tomography. *Nucl Med Commun* 1999; 20: 505-10.
7. Versijpt J, Decoo D, Van Laere KJ et al. ^{57}Co SPECT, ^{99m}Tc-ECD SPECT, MRI and neuropsychological testing in senile dementia of the Alzheimer type. *Nucl Med Commun* 2001; 22: 713-9.
8. Johnson KA, Kijewski MF, Becker JA et al. Quantitative brain SPECT in Alzheimer's disease and normal aging. *J Nucl Med* 1993; 34: 2044-8.
9. Tanaka F, Vines D, Tsuchida T et al. Normal patterns on ^{99m}Tc-ECD brain SPECT scans in adults. *J Nucl Med* 2000; 41: 1456-64.
10. Morano GN, Seibyl JP. Technical overview of brain SPECT imaging: improving acquisition and processing of data. *J Nucl Med Technol* 2003; 31: 191-5.
11. Kalantari F, Rajabi H, Saghari M. Quantification and reduction of attenuation related artifacts in SPET by applying attenuation model during iterative image reconstruction: A Monte Carlo study. *Hell J Nucl Med* 2011; 14: 278-83.
12. Zhang JJ, Park CH, Kim SM et al. The attenuation effect in brain SPECT. *Clin Nucl Med* 1993; 18: 583-6.
13. Warwick JM, Rubow S, du Toit M et al. The Role of CT-Based Attenuation Correction and Collimator Blurring Correction in Striatal Spect Quantification. *Int J Mol Imaging* 2011; 2011: 195037. Epub 2011 Apr 6.
14. Gustafsson A, Arlig A, Jacobsson L et al. Dual-window scatter correction and energy window setting in cerebral blood flow SPECT: a Monte Carlo study. *Phys Med Biol* 2000; 45: 3431-40.
15. Mas J, Ben Younes B, Bidet R. Improvement of quantification in SPECT studies by scatter and attenuation compensation. *Eur J Nucl Med* 1989; 15: 351-6.
16. Kim KM, Varrone A, Watabe H et al.Contribution of scatter and attenuation compensation to SPECT images of nonuniformly distributed brain activities. *J Nucl Med* 2003; 44: 512-9.
17. Kalantari F, Rajabi H, Saghari M. Quantification and reduction of the collimator-detector response effect in SPECT by applying a system model during iterative image reconstruction: a simulation study. *Nucl Med Commun* 2012; 33: 228-38.
18. Ghoorun S, Baete K, Nuyts J et al. The influence of attenuation correction and reconstruction techniques on the detection of hypo-perfused lesionsin brain SPECT images. *Nucl Med Commun* 2006; 27: 765-72.
19. King MA, Schwinger RB, Doherty PW, Penney BC. Two-dimensional filtering of SPECT images using the Metz and Wiener filters. *J Nucl Med* 1984; 25: 1234-40.
20. Raeisi E, Rajabi H, Aghamiri SMR. A New Approach for Quantitative Evaluation of Reconstruction Algorithms in SPECT. *Iranian J Rad Res* 2006; 4: 77-80.
21. Arlig A, Gustafsson A, Jacobsson L et al. Attenuation correction in quantitative SPECT of cerebral blood flow: a Monte Carlo study. *Phys Med Biol* 2000; 45: 3847-59.
22. Hayashi M, Deguchi J, Utsunomiya K et al.Comparison of methods of attenuation and scatter correction in brain perfusion SPECT. *J Nucl Med Technol* 2005; 33: 224-9.
23. Stodilka RZ, Kemp BJ, Msaki P et al. The relative contributions of scatter and attenuation corrections toward improved brain SPECT quantification. *Phys Med Biol* 1998; 43: 2991-3008.
24. Farid K, Habert MO, Martineau A et al. CT nonuniform attenuation and TEW scatter corrections in brain ^{99m}Tc-ECD SPECT. *Clin Nucl Med* 2011; 36: 665-8.
25. King MA, Penney BC, Glick SJ. An image-dependent Metz filter for nuclear medicine images. *J Nucl Med* 1988; 29: 1980-9.
26. King MA, Doherty PW, Schwinger RB, Penney BC. A Wiener filter for nuclear medicine images. *Med Phys* 1983; 10: 876-80.
27. Floyd CE, Jr., Jaszczak RJ, Greer KL, Coleman RE. Inverse Monte Carlo as a unified reconstruction algorithm for ECT. *J Nucl Med* 1986; 27: 1577-85.
28. Tsui BMW, Gullberg GT, Hu HB. Incorporation of detector response in projector and backprojector for SPECT image reconstruction. *J Nucl Med* 1987; 28: 566.
29. Zeng GL, Gullberg GT. Three-Dimensinal Iterative Reconstruction Algorithms With Attenuation And Geometric Point Response Correction. *IEEE Trans Nucl Sci* 1991; 38: 693-702.
30. Tsui BMW, Frey EC, Zhaot X et al. The importance andimplementation of accurate 3D compensation methods for quantitative SPECT. *Phys Med Biol* 1994; 39: 509-30.
31. Hudson HM, Larkin RS. Accelerated image reconstruction using ordered subsets of projection data. *IEEE Trans Med Imag* 1994; 13: 601-19.
32. Shepp LA, Vardi Y. Maximum Likelihood Reconstruction for Emission Tomography. *IEEE Trans Med Imag* 1982; 1: 113-22.
33. Yokoi T, Shinohara H, Onishi H. Performance evaluation of OSEM reconstruction algorithm incorporating three-dimensional distance-dependent resolution compensation for brain SPECT: a simulation study. *Ann Nucl Med* 2002; 16: 11-8.
34. Zubal IG, Harrell CR, Smith EO et al. Computerized three-dimensional segmented human anatomy. *Med Phys* 1994; 21: 299-302.
35. Green P. Bayesian reconstructions from emission tomography data using a modified EM algorithm. *IEEE Trans Med Imag* 1990; 9: 84-93.
36. Imon Y, Matsuda H, Ogawa M et al. SPECT image analysis using statistical parametric mapping in patients with Parkinson's disease. *J Nucl Med* 1999; 40: 1583.
37. Chang LT. A method for attenuation correction in radionuclide computed tomography. *IEEE Trans Nucl Sci* 1978; 25: 638-43.
38. Cot A, Falcσn C, Crespo C et al. Absolute quantification in dopaminergic neurotransmission SPECT using a Monte Carlo-based scatter correction and fully 3-dimensional reconstruction. *J Nucl Med* 2005; 46: 1497-504.
39. Crespo C, Gallego J, Cot A et al. Quantification of dopaminergic neurotransmission SPECT studies with ^{123}I-labelled radioligands. A comparison between different imaging systems and data acquisition protocols using Monte Carlo simulation. *Eur J Nucl Med Mol Imag* 2008; 35: 1334-42.
40. Catafau AM, Bullich S, Danús M et al. Test-retest variability and reliability of ^{123}I-IBZM SPECT measurement of striatal dopamine D_2 receptor availability in healthy volunteers and influence of iterative reconstruction algorithms. *Synapse* 2008; 62: 62-9.
41. Bullich S, Cot A, Gallego J et al. Impact of scatter correction on D_2 receptor occupancy measurements using ^{123}I-IBZM SPECT: comparison to C-Raclopride PET. *Neuroimage* 2010; 50: 1511-8.
42. Arosio M, Pasquali C, Crivellaro C et al. Performance of a SPECT collimator-detector response reconstruction algorithm: phantom studies and validation in inflammation clinical studies. *Q J Nucl Med Mol Imaging* 2011; 55: 671-9.
43. Venero CV, Heller GV, Bateman TM et al. A multicenter evaluation of a new post-processing method with depth-dependent collimator resolution applied to full-time and half-time acquisitions without and with simultaneously acquired attenuation correction. *J Nucl Cardiol* 2009; 16: 714-25.